Advances in Differential Equations and Control Processes 2026, 33(3), 4390.
doi: https://doi.org/10.59400/adecp4390

Article

Not loss of stability but steady-state shift: A systems biology explanation for elevated fasting blood glucose in type 2 diabetes

Guanyu Wang[1,2,3]

[1] Laboratory of Biocomplexity and Engineering Biology, Department of Biomedical Engineering, School of Medicine, The Chinese University of Hong Kong, Shenzhen 518172, China; wangguanyu@cuhk.edu.cn

[2] CUHKSZ-STEM Joint Laboratory of Precision Medicine, The Chinese University of Hong Kong, Shenzhen 518172, China

[3] Ciechanover Institute of Precision and Regenerative Medicine, School of Medicine, The Chinese University of Hong Kong, Shenzhen 518172, China

CITATION

Wang G. Not loss of stability but steady-state shift: A systems biology explanation for elevated fasting blood glucose in type 2 diabetes. Advances in Differential Equations and Control Processes. 2026; 33(3): 4390. https://doi.org/10.59400/adecp4390

ARTICLE INFO

Received: 12 May 2026
Revised: 17 June 2026
Accepted: 23 June 2026
Available online: 3 July 2026

Abstract: Elevated fasting blood glucose is a hallmark clinical feature of prediabetes and type 2 diabetes, reflecting underlying pathological alterations in the body's glucose-insulin regulatory system. This study employs a validated mathematical model of the glucose-insulin negative feedback loop to investigate the fundamental mechanisms of this elevation from a systems biology perspective. We specifically analyzed whether hyperglycemia arises from decreased system stability or an upward shift in the steady-state set-point. Our findings demonstrate that the intrinsic stability of the glucose-insulin regulatory system remains largely unchanged from healthy states through early-stage diabetes. Contrary to the hypothesis of stability decay, the essence of elevated fasting glucose is an upward shift of the steady-state level driven primarily by hepatic insulin resistance, which increases basal hepatic glucose output. While system stability is preserved during early progression, the dynamic coupling between glucose and insulin weakens; low-frequency oscillations inherent to the healthy system gradually diminish and eventually disappear as insulin resistance intensifies, signaling a decoupling of dynamics before stability loss. Significant weakening of system stability, characterized by a markedly reduced convergence rate following perturbation, occurs only in late-stage diabetes accompanied by severe pancreatic damage and compromised insulin secretory capacity. These results redefine the pathophysiological understanding of fasting hyperglycemia, suggesting that early therapeutic strategies should target recalibrating the glucose set point and hepatic sensitivity rather than bolstering system stability. This research provides valuable theoretical insights into the pathogenesis of diabetes and highlights potential dynamic biomarkers for monitoring disease progression.

Keywords: glucose-insulin regulatory system; diabetes; prediabetes; stability analysis; systems biology

1. Introduction

Elevated fasting blood glucose is a hallmark clinical feature of prediabetes and type 2 diabetes [1], reflecting underlying pathological alterations in the body's glucose-insulin regulatory system. In healthy individuals, glucose homeostasis is maintained through precisely coordinated regulation involving multiple hormones (including insulin and glucagon) and organs (including the liver, muscle, and adipose tissue). Given its straightforward measurement and reliable outcomes, fasting blood

glucose has become a core indicator for type 2 diabetes screening and routine health examinations [2], making the elucidation of its pathological mechanisms both scientifically valuable and clinically important.

From a systems biology perspective, elevated fasting blood glucose may arise through two potential mechanisms: (1) Decreased system stability, wherein weakened feedback regulatory capacity causes glucose to deviate from homeostasis and gradually elevate [3]; or (2) Upward shift of the steady state, wherein system stability remains intact, but the body establishes a higher glucose set-point [4]. If the latter mechanism prevails, further investigation is warranted to identify the driving factors behind this set-point elevation. As elevated fasting blood glucose serves as an early marker and key indicator of obesity and diabetes-related disease progression, in-depth analysis of these scientific questions not only clarifies whether glucose homeostasis imbalance stems from system stability decay or set-point recalibration, but also provides a theoretical foundation for elucidating diabetic pathogenic mechanisms and developing targeted therapeutic strategies.

Mathematical models offer the advantage of integrating multiple factors within a unified framework, thereby yielding more comprehensive and reliable conclusions [5]. Building upon a validated mathematical model of the glucose-insulin negative feedback regulatory system, this study addresses the aforementioned scientific questions. Our findings reveal that the stability of the body's glucose regulatory system remains largely invariant across health states; elevated fasting blood glucose results from an upward shift of the set-point driven by hepatic insulin resistance. Throughout disease progression, the degree of system stability (defined as the convergence rate of the state point to the set-point following perturbation) remains essentially unchanged. Only in late-stage diabetes with severe pancreatic damage does system stability exhibit significant weakening, though a certain degree of stability is still maintained.

Beyond addressing diabetes-related scientific questions, this study also elucidates the dynamic characteristics of the glucose-insulin system in the fasting state. When the system is perturbed, deviations in glucose and insulin gradually decay due to inherent system stability. This decay is accompanied by in-phase oscillations of glucose and insulin, reflecting the profound coupling between their dynamics. Due to their relatively low frequency, these oscillations are not readily observable. As diabetes progresses, although system stability remains largely unchanged over an extended range, this oscillatory characteristic markedly weakens until oscillations disappear entirely, resulting in complete decoupling of glucose and insulin dynamics.

2. Materials and methods

2.1. Mathematical model

This study employs a validated mathematical model of the glucose-insulin negative feedback regulatory system, building upon previous validation studies [6–8]:

$$\frac{dG}{dt} = \frac{S_{hep}(I) + S_{oral}}{\Omega} - \gamma G - V(I)G, \tag{1}$$

$$\frac{dI}{dt} = f(G) - k \cdot I, \tag{2}$$

where

$G(t)$ is the plasma glucose concentration.

$I(t)$ is the plasma insulin concentration.

$S_{hep}(I(t))$ is the rate of endogenous glucose (secreted by the liver) appearing in the blood [9]. Because insulin inhibits hepatic glucose production, $S_{hep}(I)$ is a decreasing function of I (e.g., **Figure 1a**). To model $S_{hep}(I)$, an exponential decay model is usually used [10–13]:

$$S_{hep}(I) = S_{basal} exp\left[-\alpha\left(I - I_{basal}\right)\right] + S_{res}, \tag{3}$$

where S_{basal} is the basal hepatic glucose output rate; S_{res} is the residual hepatic glucose output; α is the hepatic insulin sensitivity coefficient [14]; I_{basal} is the basal insulin concentration.

$S_{oral}(t)$ is the rate of oral glucose appearing in the blood [9].

Ω is the blood volume per kg body weight [15].

γ is the rate of basal (non-insulin-dependent) glucose utilization per unit glucose concentration. It is primarily contributed by the brain.

$V(I(t))$ is the rate of insulin-mediated glucose disposal per unit glucose concentration (**Figure 1b**).

k is the rate of insulin degradation.

$f(G(t))$ is the rate of insulin secretion in response to glucose stimulation (**Figure 1c**). As in the study by Wang [7], it is modeled by a Hill function

$$f(G) = f_{max}\text{Hill}\left(\frac{G}{G_h}\right) \tag{4}$$

with

$$\text{Hill}(x) = \frac{x^n}{1 + x^n}, \tag{5}$$

where $f_{\max}$ is the maximal rate; G_h is the EC_{50} glucose concentration; n is the Hill coefficient [16].

In the fasting steady state, the glucose and insulin concentrations are denoted by G_0 and I_0, respectively.

2.2. Parameter values

The parameter values of the mathematical model (Equations (1) and (2)) are obtained as follows.

Parameter Ω: Approximately 0.075 L/(kg body weight) [8,17]. Thus, the unit of $(S_{hep} + S_{oral})/\Omega$ is mM/min, which represents the rate of total glucose appearing in the blood.

Parameter k: This is the rate of insulin degradation. In the fasting state, insulin is primarily degraded in the liver, so the k value depends on the degradation rate of insulin in the liver. In the fasting state, the half-life of insulin in plasma is τ = 4–6 min [18], which means the normal range of $k = \ln(2)/\tau$ is 0.12–0.17 min^{-1}. In the following, the intermediate value k = 0.145 is used whenever a fixed value of k is needed.

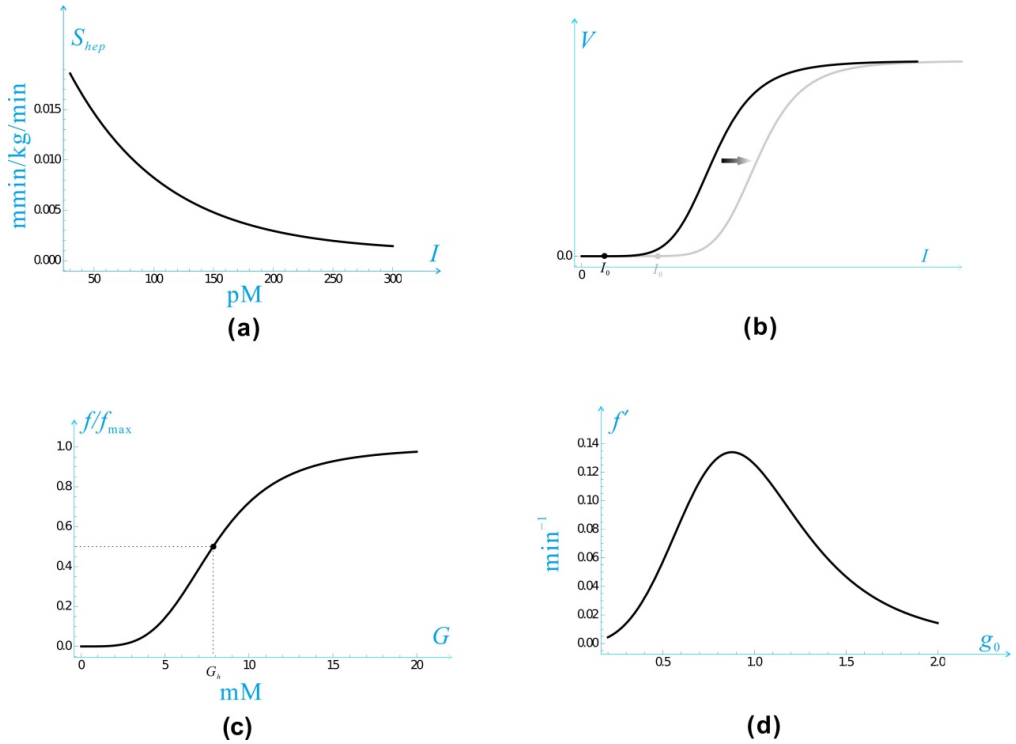

Figure 1. **(a)** $S_{hep}(I)$, the rate of endogenous glucose appearing in the blood as a function of insulin concentration. **(b)** $V(I)$, the rate of insulin-mediated glucose disposal per unit glucose concentration as a function of insulin concentration. **(c)** $f(G)$, the rate of insulin secretion in response to glucose stimulation. **(d)** f' as a function of g_0.

Note: Here f' denotes the derivative of f with respect to G, evaluated at G_0 (see Equation (16)). By defining $g_0 = \frac{G_0}{G_h}$, f' is then expressed as a function of g_0 (see Equation (A3)).

Parameter γ: This represents the rate of insulin-independent glucose utilization. Since this primarily reflects the rate at which the brain extracts blood glucose, it should be minimally affected by diabetes-related conditions. We validated this hypothesis using data from the literature [9]. Mitrakou et al. [9] conducted an oral glucose tolerance test (OGTT) on four groups of human subjects: DB^-OB^- (Group 1), DB^-OB^+ (Group 2), DB^+OB^- (Group 3), and DB^+OB^+ (Group 4), where DB and OB denote diabetes and obesity, respectively. Notably, lower group numbers correspond to healthier subjects. During OGTT, the $S_{hep}(I_0)$ and G_0 values for all four groups were directly measured, as shown in the second and third rows of **Table 1**, respectively. Using Equation (6), the γ values for each group were calculated and are presented in the fourth row of **Table 1**. The results demonstrate that γ values across all four groups remain approximately 0.025 min^{-1}. In other words, although the subject's health status progressively declined from Group 1 to Group 4, the rate of cerebral glucose extraction showed no significant change, consistent with our expectations. Furthermore, using an alternative dataset [19] and a different methodology, we independently arrived at the same conclusion: $\gamma \approx 0.025$ min^{-1} [7].

Table 1. Some clinical data [9].

Group	**DB^-OB^-**	**DB^-OB^+**	**DB^+OB^-**	**DB^+OB^+**
$S_{hep}(I_0)$ (mmol/min/kg)	0.011	0.011	0.0118	0.011
G_0 (mM)	5.5	5.85	6.00	6.10
γ (min^{-1})	0.0265	0.0250	0.0262	0.0242

Regarding the $S_{hep}(I)$ function: The approximate ranges for S_{basal}, S_{res}, α, and I_{basal} are 2.0–2.4 mg/min/kg, 0.1–0.2 mg/min/kg, 0.05–0.1 mL/μU, and 10 μU/mL, respectively [10–13]. Given that the molar mass of glucose is 180 g/mol and 1μU/mL insulin corresponds to 6 pM [20], these parameters can be converted to the following ranges: S_{basal} = 0.0111–0.0133 mmol/min/kg, S_{res} = 0.000556–0.00111 mmol/min/kg, α = 0.0083–0.0167 pM^{-1}, and I_{basal} = 60 pM.

Regarding the $f(G)$ function: The value of G_h is set to 7.86 mM [21, 22]. To determine the other two parameters, $f_{\max}$ and n, two algebraic equations are required. These can be derived by applying Equation (7) twice: first, using the lower limits of G_0 (4 mM) and I_0 (30 pM); second, using the upper limits of G_0 (6 mM) and I_0 (120 pM). From the two algebraic equations, we obtain: $f_{\max}$ = 71.6 pM/min and n = 3.951.

The parameter values and their normal ranges are presented in **Table 2**.

Table 2. Parameter values of the mathematical model.

Parameter	Value	Normal range	Unit
Ω	0.075	—	L/kg
k	0.145	0.12–0.17	min^{-1}
γ	0.025	0.024–0.027	min^{-1}
S_{basal}	1.22×10^{-2}	1.11–1.33 ($\times 10^{-2}$)	mmol/min/kg
S_{res}	8.33×10^{-4}	5.56–11.1 ($\times 10^{-4}$)	mmol/min/kg
α	12.5×10^{-3}	8.3–16.7 ($\times 10^{-3}$)	pM^{-1}
I_{basal}	60	—	pM
G_h	7.86	—	mM
$f_{\max}$	71.6	—	pM/min
n	3.951	—	dimensionless
G_0	To be determined	4–6	mM
I_0	To be determined	30–120	pM

3. Results and discussion

3.1. Steady state analysis

During fasting, there is no food ingestion, i.e., $S_{oral}(t) \equiv 0$. The rate of insulin-mediated glucose disposal is approximately zero ($V(I_0) \approx 0$, indicated by the black point in **Figure 1a**. This occurs because insulin-responsive tissues, such as muscle and adipose tissue, minimize glucose extraction during fasting, thereby prioritizing the limited blood glucose supply for the brain [23, 24]. For insulin-responsive tissues such as muscle and adipose, each cell has an insulin response threshold [6–8]. Glucose extraction by these cells initiates only when the plasma insulin concentration is sufficiently high to exceed this threshold. Since the fasting insulin concentration I_0 is substantially below the threshold of all insulin-responsive cells, none of these cells extract blood glucose during fasting. At the organism level, this manifests as the $V(I)$ curve exhibiting zero V values over a wide range of insulin concentrations, with I_0 falling precisely within this range. In contrast, organs or tissues not regulated by insulin (primarily the brain) continue to extract blood glucose at a rate of γ during the fasting state.

In the steady state, dG/dt = 0 and dI/dt = 0, which reduce the ODEs to algebraic

equations:

$$G_0 = \frac{S_{hep}(I_0)}{\gamma \cdot \Omega}, \tag{6}$$

$$I_0 = \frac{f(G_0)}{k}. \tag{7}$$

Using the parameter values listed in **Table 2**, Equations (6) and (7) were solved, yielding G_0 = 5.263 mM and I_0 = 84.02 pM. These values fall within the normal physiological ranges of 4–6 mM and 30–120 pM, respectively, demonstrating that they represent reasonable solutions.

3.2. Stability analysis reveals that the glucose-insulin system is always stable

The Jacobian matrix J at the steady state (G_0, I_0) is shown in Equation (A1). In **Appendix A**, we show that J can be simplified into:

$$J = \begin{bmatrix} -\gamma & \frac{S'}{\Omega} \\ f' & -k \end{bmatrix}, \tag{8}$$

from which the eigenvalues are solved:

$$\lambda_1 = \frac{-(k+\gamma) + \sqrt{\Delta}}{2} \tag{9}$$

and

$$\lambda_2 = \frac{-(k+\gamma) - \sqrt{\Delta}}{2}, \tag{10}$$

where

$$\Delta = (k-\gamma)^2 + \frac{4S'f'}{\Omega} \tag{11}$$

is the discriminant. Because $S_{hep}(I)$ (**Figure 1a**) and $f(G)$ (**Figure 1c**) are decreasing and increasing functions, respectively, S' and f' are negative and positive, respectively. Therefore, $S'f'$ is negative, which makes it possible that Δ is negative.

- If Δ is negative, then λ_1 and λ_2 are conjugate complex numbers with negative real parts, and the system is thus stable.
- If Δ is non-negative, then $\sqrt{\Delta}$ is real. Because $S'f'$ is negative,

$$\sqrt{\Delta} \leq \sqrt{(k-\gamma)^2} = k - \gamma. \tag{12}$$

Thus,

$$\lambda_1 \leq \frac{-(k+\gamma) + (k-\gamma)}{2} = -\gamma \tag{13}$$

and

$$\lambda_2 \leq \frac{-(k+\gamma) - (k-\gamma_0)}{2} = -k. \tag{14}$$

Therefore, λ_1 and λ_2 are both negative real numbers, and the system is again stable.

In conclusion, the glucose-insulin system exhibits strong intrinsic stability, which depends on the structural architecture of the system itself rather than on specific

parameter values. Whether in healthy individuals, sub-healthy states, or diabetic conditions, the glucose-insulin system maintains robust stability.

3.3. The degree of stability under physiologic conditions

We estimate the degree of stability in the healthy state by numerically calculating the range of eigenvalues. In the expression of Δ (Equation (11)), k and γ are relatively constant; therefore, changes in the degree of system stability are primarily determined by S' (reflecting hepatic sensitivity to insulin) and f'(reflecting pancreatic sensitivity to glucose)—two quantities susceptible to disease-related alterations.

For S', we obtain from Equation (3) that:

$$S' = -\alpha S_{basal} exp\left[-\alpha\left(I_0 - I_{basal}\right)\right]. \tag{15}$$

Based on the normal parameter ranges (**Table 2**), the normal range of S' is determined to be $-3.67 \times 10^{-4} - 5.67 \times 10^{-5}$ L/min/kg.

For f', we obtain from Equation (4) that:

$$f' = \frac{nf\left(G_0\right)}{G_0}\left[1 - \frac{f\left(G_0\right)}{f_{max}}\right]. \tag{16}$$

Based on the normal parameter ranges (**Table 2**), the normal range of f' is determined to be 4.29–8.98 min^{-1}.

Therefore, the normal range of $\frac{4S'f'}{\Omega}$ should be −0.194 to −0.013 min^{-2}. Combined with the normal range of $(k-\gamma)^2$ being 0.009 to 0.021 min^{-2}, we obtain a normal range of Δ from −0.185 to 0.008. The actual range should be significantly narrower than this estimate, as this calculation treats the parameters as independent when they are, in fact, correlated. Therefore, in the healthy state, Δ should be a negative number with an absolute value less than 0.18; the two eigenvalues $\lambda_{1,2} = \frac{-(k+\gamma)}{2} \pm \frac{i\sqrt{-\Delta}}{2}$ are conjugate complex numbers, where the real part $-(k + \gamma)/2$ is approximately −0.085 min^{-1} and the imaginary part $\frac{\sqrt{-\Delta}}{2}$ is in the range 0–0.2 min^{-1}.

These numerical calculation results are consistent with the conclusions of the mathematical analysis presented in the previous section, indicating that the glucose-insulin regulatory system exhibits strong stability. Since Δ is negative, the eigenvalues are conjugate complex numbers, which implies that state deviations following perturbation will decay exponentially (with a decay half-life of approximately $\ln(2)/0.085 \approx 8$ min) and be accompanied by oscillations (with an oscillation period greater than $2\pi/0.2 \approx 31.4$ min). However, these oscillations are too slow relative to the decay rate; by the time one oscillation cycle completes, the deviation has already decayed to near zero, making the oscillations difficult to observe experimentally. Additionally, the condition $\Delta < 0$ results in deep coupling between glucose and insulin dynamics; their respective deviations decay at the same rate and oscillate at the same frequency. Furthermore, the decay rate remains relatively consistent across different individuals (half-lives are all approximately 8 min), whereas the oscillation frequency may exhibit greater inter-individual variation (oscillation periods exceed 31.4 min).

3.4. The degree of stability under type 2 diabetes inducing factors

Although the glucose-insulin system remains stable across all conditions, its degree of stability may weaken as health status deteriorates. The parameters k and γ remain relatively constant; in contrast, S' and f' exhibit substantially greater variability. Since S' and f' are embedded within Δ, the discriminant Δ serves as the primary variable influencing the degree of stability. Through the transformations presented in **Appendix B**, we find that the discriminant Δ is primarily determined by three adjustable parameters: $\widehat{\alpha}$, i_0, and g_0. That is:

$$\Delta(\widehat{\alpha}, g_0, i_0) = 0.0144 - \frac{0.3903\widehat{\alpha}\text{Hill}(g_0)[1-\text{Hill}(g_0)]\,exp[-\widehat{\alpha}(i_0-1)]}{g_0}. \quad (17)$$

To illustrate $\Delta(\widehat{\alpha}, g_0, i_0)$, we sampled several discrete i_0 values: i_0 = 0.1, 0.5, 1.0, 2.0, 3.0. For each i_0 value, we determined its corresponding $\Delta(\widehat{\alpha}, g_0)$ and plotted the resulting graph.

We first consider the normal case of i_0 = 1.0 (when I_{basal} = 60 pM, I_0 is also 60 pM, representing a standard fasting insulin concentration). We have:

$$\Delta(\widehat{\alpha}, g_0, 1) = 0.0144 - \frac{0.3903\widehat{\alpha}\text{Hill}(g_0)[1-\text{Hill}(g_0)]}{g_0}, \quad (18)$$

whose graph is shown in **Figure 2c**, where $\widehat{\alpha}$ ranges over [0.05, 5.0] and g_0 ranges over [0.1, 2.0]. **Figure 2f** shows the corresponding contour plot. Similar to the normal physiology scenario, Δ is negative for almost all the $\widehat{\alpha}$ and g_0 values. That is, as long as i_0 is normal (e.g., i_0 = 1.0), even if the subject is in a severe pathologic state, the dynamic characteristics of the system most likely remain the same as in the healthy condition (exponential decay accompanied by oscillations).

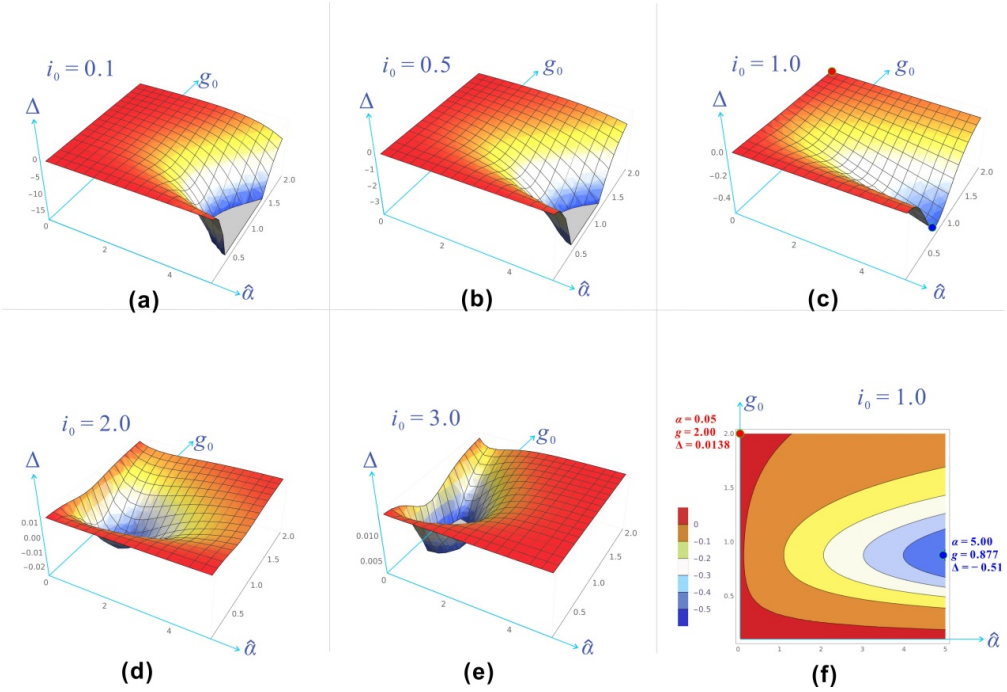

Figure 2. Δ as a function of $\widehat{\alpha}$ and g_0 when i_0 = 0.1 **(a)**, 0.5 **(b)**, 1.0 **(c)**, 2.0 **(d)**, and 3.0 **(e)**. When i_0 = 1.0, the contour plot is also shown **(f)**.

The red point in **Figure 2** represents an exception, as it exhibits the maximum Δ value ($\Delta = 0.0138$). Since $\Delta > 0$, the eigenvalues are no longer conjugate complex numbers, indicating the absence of oscillations. Because $\Delta \approx 0$, one obtains $\lambda_1 \approx \lambda_2 \approx -(k + \gamma)/2$ based on Equations (9) and (10), indicating that the degree of stability remains virtually unchanged as Δ transitions from negative to positive. That is, even for a pathologic state such as the red point, the degree of system stability is similar to that in the healthy state; only the oscillations vanish. The red point represents a pathologic state due to its minimum value ($\widehat{\alpha} = 0.05$), which indicates an extremely low hepatic insulin sensitivity coefficient. This corresponds to severe hepatic insulin resistance, a hallmark of type 2 diabetes. Thus, the phenomenon of oscillation disappears only under theoretical limit conditions.

The blue point in **Figure 2** exhibits the maximum $\widehat{\alpha}$ value ($\widehat{\alpha} = 5.0$), representing extreme hepatic sensitivity to insulin. Its Δ value is the most negative ($|\Delta| = 0.51$), corresponding to the highest oscillation frequency (frequency = $\frac{\sqrt{-\Delta}}{4\pi} = 0.057$ min^{-1}; period = 17.6 min).

In summary, hepatic insulin sensitivity significantly affects oscillations during system convergence, although it has minimal effect on the degree of system stability. When hepatic sensitivity is extremely high ($\widehat{\alpha} = 5.0$), the oscillation period can be as short as 17.6 min. As insulin sensitivity decreases, the oscillation frequency progressively diminishes. When $\widehat{\alpha} = 0.75$ (the healthy state described in the previous section), the oscillation period increases to 31.4 min. Under extreme insulin resistance conditions ($\widehat{\alpha} = 0.05$), $\Delta = 0.0138$ becomes positive, indicating the system oscillations completely disappear, and glucose and insulin dynamics become fully decoupled. As shown in **Figure 2f**, the parameter g_0 has a lesser effect on the Δ value, with significant effects observed only when $\widehat{\alpha}$ exceeds 1.

When i_0 becomes smaller (**Figure 2a,b**), Δ becomes increasingly negative, indicating that the degree of system stability remains unchanged while oscillations intensify. When i_0 reaches an extreme value of 0.1 (**Figure 2a**), for example, the minimum Δ is -46.8, corresponding to an extremely high oscillation frequency of 0.54 min^{-1} (period = 1.85 min). However, such a high frequency of glucose-insulin oscillation would never happen in reality, as $i_0 = 0.1$ is physiologically unrealistic.

When i_0 becomes larger (**Figure 2d,e**), increasingly positive Δ values appear, but these positive values are all very small, approximately equal to zero. For example, when $i_0 = 2.0$, most Δ values remain negative, but some Δ values become positive. The maximum Δ value is $\Delta(0.05, 2.0, 2.0) = 0.0139$, nearly identical to the maximum value of 0.0138 when $i_0 = 1.0$. That is, even when Δ becomes positive, it remains approximately equal to 0. When $i_0 = 3.0$, almost all Δ values are positive, as the minimum Δ value is $\Delta(0.5, 0.877, 3.0) = -0.0047$, which is already close to 0. However, the maximum Δ value is $\Delta(4.523, 1.301, 3.0) = 0.0144$, also close to 0. In summary, the increase in i_0 causes Δ to tend toward positive values, the oscillation amplitude of the system tends to disappear, and the dynamics of glucose and insulin tend to decouple. However, even for extreme $\widehat{\alpha}$, g_0, and i_0 values, the absolute value of positive Δ remains very small, close to 0, so it has virtually no effect on the degree of stability. Any deviation still decays at a rate of $\lambda_1 \approx \lambda_2 \approx -(k + \gamma)/2$.

In the above analysis, $f_{\max}$ was fixed at a normal value of 80.8, meaning that the maximum capacity of the pancreas secreting insulin remained intact. However, when diabetes progresses to an advanced stage, the pancreas becomes damaged due to excessive insulin secretion, resulting in a significant decline in its insulin secretory capacity [25]—that is, $f_{\max}$ becomes substantially reduced. Under these conditions, how will the stability of the glucose-insulin system change?

To address this question, we first consider the limiting case $f_{\max} = 0$, i.e., assuming the pancreas completely loses its insulin-producing capacity. In this case, $f' = 0$ and $\Delta = k - \gamma$. Therefore, $\lambda_1 = -\gamma$ and $\lambda_2 = -k$, implying that the dynamics of glucose and insulin are completely decoupled. Since $\gamma = 0.025$ is substantially smaller than $k = 0.145$, the stability of glucose is markedly weakened while that of insulin is considerably strengthened; consequently, the overall stability is diminished. Notably, the above analysis pertains to the limiting case $f_{\max} = 0$. Even under this most severe pathological condition (complete pancreatic damage), the system remains stable, albeit with completely decoupled glucose and insulin dynamics. As $f_{\max}$ increases from zero, the glucose and insulin dynamics become progressively coupled until the two eigenvalues converge ($\lambda_1 = \lambda_2 = -(k + \gamma)/2$), at which point the degree of stability reaches its maximum. With further increases in $f_{\max}$, the coupling between glucose and insulin intensifies (manifested as the onset of oscillations), while the overall degree of stability remains essentially unchanged.

3.5. The elevation of fasting blood glucose concentration is due to the upward shift of steady-state

The gradual elevation of fasting blood glucose concentration G_0 already occurs in prediabetes and early diabetes. Since the above analysis demonstrates that early disease progression generally does not alter the degree of system stability, what exactly causes the gradual elevation of fasting blood glucose concentration?

In Equation (6), γ and Ω are rather constant; thus, the elevation of fasting blood glucose concentration should be attributed to the gradual increase in $S_{hep}(I_0)$. In the expression of S_{hep} (Equation (3)), there are four parameters: S_{basal}, I_{basal}, S_{res}, and α. Because S_{basal}, I_{basal}, and S_{res} remain relatively constant, hepatic insulin sensitivity α should be the primary factor affecting G_0.

As is well established, insulin resistance is the pathological basis of type 2 diabetes [26], and it is generally agreed that hepatic insulin resistance precedes muscle insulin resistance [9,12,27]. Even in patients with mild diabetes or prediabetes, hepatic insulin resistance is already significant and highly correlated with fasting blood glucose levels [28]. In contrast, the degree of peripheral resistance correlates weakly with fasting blood glucose and is more closely associated with postprandial blood glucose. In the natural history of the disease, slight elevation of fasting blood glucose often precedes obvious postprandial blood glucose abnormalities (although the two often overlap) [29].

The enhancement of hepatic insulin resistance corresponds to the weakening of hepatic insulin sensitivity—that is, a decrease in α. According to Equation (3), the decrease in α causes an increase in $S_{hep}(I_0)$, and the increase in $S_{hep}(I_0)$ causes an

increase in G_0 (Equation (6)), subsequently leading to an increase in I_0 (Equation (7)). At this point, G_0 and I_0 complete a cycle of elevation. Based on our analysis in the previous section, the stability of the entire process is generally maintained; thus, the essence of G_0 and I_0 elevation is an upward shift of the steady state.

4. Discussion

As individuals reach middle and old age, with increasing age and deteriorating health status, fasting blood glucose levels generally rise gradually beyond the healthy range of 4–6 mM. A seemingly reasonable explanation for this phenomenon is that the stability of the glucose-insulin regulatory system progressively deteriorates, making blood glucose increasingly difficult to control within the normal range of 4–6 mM. However, with the aid of a validated mathematical model, we found that the glucose-insulin system remains stable throughout; even in relatively advanced diabetic stages, it can maintain approximately the same degree of stability as in the healthy state.

In the healthy state, state deviations caused by perturbation decay at a rate with a half-life of approximately 8 min, accompanied by oscillations with a period of about 30 min. As diabetes progresses (hepatic insulin resistance increases, i.e., α decreases), the decay rate of deviations remains largely unchanged, indicating that the degree of stability is preserved; however, the oscillation frequency progressively diminishes until oscillations completely disappear ($\Delta \geq 0$). Since $\Delta \approx 0$, the dynamics of glucose and insulin are not significantly decoupled; the rate constants of deviation decay for both remain approximately $-(k+\gamma)/2$, even though oscillations vanish.

In the advanced stage of diabetes, the pancreas becomes severely damaged, and its insulin secretory capacity ($f_{\max}$) declines substantially. Under these conditions, Δ becomes positive (resulting in the disappearance of oscillations) and assumes a relatively large positive value (leading to significant decoupling of glucose and insulin dynamics). The rate at which glucose returns to baseline following perturbation slows considerably, with the rate constant decreasing from $-(k+\gamma)/2$ to $-\gamma$; conversely, the rate at which insulin returns following perturbation accelerates substantially, with the rate constant increasing from $-(k+\gamma)/2$ to $-k$. That is, the degree of stability of glucose dynamics is significantly compromised, making it difficult for blood glucose to return to normal levels. Nevertheless, the system remains stable regardless (guaranteed by $-\gamma$).

There is an important caveat to the above analysis: the true eigenvalue is $-\gamma - V(I_0)$; this eigenvalue can be simplified to $-\gamma$ only when $V(I_0) \approx 0$. Under normal physiological conditions, $V(I_0) \approx 0$ certainly holds because the fasting insulin concentration I_0 is far below the insulin response threshold of cells. However, as obesity or diabetes pathology progresses, insulin concentrations increase, including the fasting insulin concentration I_0. Thus, as I_0 increases, will $V(I_0)$ increase significantly and no longer be approximable as zero? The answer is no. The increase in insulin concentration represents a passive compensatory response; the underlying cause is that tissue cell insulin resistance increases (i.e., the insulin response threshold becomes elevated), necessitating increased insulin secretion by the pancreas for compensation. This mechanism is well illustrated in **Figure 1a**. With the progression of type 2 diabetes

pathology, I_0 increases substantially (from the black point to the gray point), but $V(I)$ as a whole also undergoes a rightward shift (from the black curve to the gray curve). In fact, $V(I)$ shifts rightward first, subsequently forcing insulin concentration to increase. As obesity and type 2 diabetes progress, the insulin response curve shifts rightward; this is a well-documented phenomenon, widely attributed to progressively intensifying insulin resistance [19,30,31]. Finally, it must be noted that I_0 does not always increase; when diabetes becomes very severe and causes pancreatic damage, the pancreas's insulin secretory capacity declines substantially, resulting in a marked decrease in I_0 [32]. In any case, $V(I_0) \approx 0$ holds regardless of the health state of the body.

Since the stability of the glucose-insulin regulatory system remains unchanged, why does the fasting blood glucose concentration G_0 gradually increase? In Equation (6), neither γ nor Ω changes; thus, the only explanation for the increase in G_0 is the increase in $S_{hep}(I_0)$—that is, the liver secretes progressively more glucose. Given that S_{hep} is a decreasing function of I_0, this phenomenon is readily explained.

The first reason is the exacerbation of hepatic insulin resistance, manifested as abnormalities in the insulin signal transduction pathway of hepatocytes, leading to weakened inhibitory effects of insulin on hepatic gluconeogenesis and glycogenolysis, and increased hepatic glucose output—which is the primary driving factor for elevated fasting blood glucose. Under physiological conditions, the liver is highly sensitive to inhibition by I_0, resulting in glucose release at a very low rate (S_{hep} is very small). Under pathological conditions, hepatic insulin resistance is significantly enhanced, meaning the liver's inhibitory response to I_0 becomes sluggish, causing S_{hep} to increase substantially. According to Equation (6), this leads to an increase in G_0—that is, elevated fasting blood glucose concentration.

The second reason is islet β-cell dysfunction, manifested as insufficient basal insulin secretion (I_0 decreases), which weakens the inhibitory capacity on hepatic glucose output. For example, when type 2 diabetes becomes very severe, the pancreas becomes damaged and cannot secrete sufficient insulin.

This study reveals a low-frequency oscillation phenomenon. Due to its slow frequency, perturbations decay substantially before the oscillation waveform emerges, making it difficult to detect—which explains why this mechanism has not been reported in prior literature. Although passive observation is unlikely to capture this oscillation, we do not exclude the possibility of its detection through ingeniously designed experiments in the future. If successfully observed, the oscillation frequency could serve as a biomarker for metabolic health (a decrease in frequency indicates deteriorating health status). In summary, while the oscillation reported herein is currently an incidental finding without immediate practical application, it may hold significant clinical implications in the future.

Mathematical models can integrate multiple distinct factors within a single framework, thereby yielding more reliable conclusions. While this study provides a systems-level explanation for elevated fasting glucose, several limitations inherent to the current mathematical model must be acknowledged, which also define the scope for future research. First, the current model relies on simplified assumptions regarding metabolic complexity. To isolate the core dynamics of the glucose-insulin negative

feedback loop, the model excludes several critical regulatory factors. Specifically, it does not incorporate the counter-regulatory effects of glucagon, the metabolic influence of FFAs, or the incretin effect (e.g., GLP-1), all of which play significant roles in glucose homeostasis. Furthermore, the model simplifies peripheral insulin resistance by assuming negligible insulin-mediated glucose uptake in muscle and adipose tissue during the fasting state. While this assumption is physiologically justified for healthy and early-stage diabetic conditions (where fasting insulin remains below the activation threshold of peripheral tissues), it may not fully capture the nuanced contributions of peripheral resistance in advanced disease states where compensatory hyperinsulinemia is profound. Consequently, the model may underestimate the indirect effects of peripheral resistance on hepatic glucose production mediated by free fatty acid (FFA) flux or altered substrate availability. That is, peripheral resistance may indirectly exacerbate hepatic gluconeogenesis through mechanisms such as increased FFA flux to the liver, thereby elevating fasting blood glucose [12, 33]. Second, the applicability of the established model is strictly confined to the fasting steady state. The parameters and structural assumptions (particularly $V(I_0) \approx 0$) are optimized to explain basal glucose regulation. Therefore, the current framework is not suitable for simulating postprandial glycemic dynamics, where rapid changes in glucose absorption, incretin secretion, and active peripheral glucose disposal dominate the system's behavior. Extending the model to cover the postprandial phase would require redefining the boundary conditions and incorporating time-dependent inputs for oral glucose absorption (S_{oral}) and dynamic hormonal responses that are beyond the scope of this fasting-focused analysis.

These limitations highlight specific directions for future model optimization and experimental validation. Future iterations of the model should aim to: (1) Integrate multi-hormonal regulation by incorporating glucagon kinetics and the FFA-insulin resistance axis to better quantify the interplay between hepatic and peripheral tissues; (2) Expand the temporal scope to simulate postprandial challenges, thereby allowing for a comprehensive analysis of system stability across the entire 24-hour glycemic profile; and (3) Validate the predicted low-frequency oscillations through high-resolution, long-duration clinical monitoring. While our theoretical analysis suggests that the decoupling of glucose-insulin dynamics (loss of oscillations) precedes the loss of stability, empirical confirmation of these subtle dynamic shifts in human subjects could provide novel biomarkers for early diabetic progression. Addressing these gaps will refine the quantitative accuracy of the model and enhance its utility in developing targeted therapeutic strategies that address both set-point shifts and stability decay.

5. Conclusion

In summary, the primary cause of elevated fasting blood glucose concentration is the upward shift of the set-point resulting from changes in system parameters, rather than a weakening of the degree of stability (although islet β-cell dysfunction does weaken the degree of stability while simultaneously promoting the upward shift of the set-point). These findings offer a critical paradigm shift in our understanding of diabetic pathogenesis. Clinically, they suggest that early therapeutic interventions should

prioritize recalibrating the glucose set-point—specifically by targeting hepatic insulin sensitivity—rather than attempting to restore a theoretically "lost" system stability. Additionally, the predicted disappearance of low-frequency oscillations provides a novel theoretical framework for identifying dynamic biomarkers of metabolic health. Future efforts to integrate multi-hormonal counter-regulation and postprandial dynamics into this modeling framework will further enhance our understanding of glucose homeostasis and aid in the development of precision interventions for type 2 diabetes.

Funding: This work was funded by the Natural Science Foundation of Guangdong grant number 2026A1515012358, the Natural Science Foundation of Shenzhen grant number JCYJ20240813113606009, and the Shenzhen Stable Support Project.

Institutional review board statement: Not applicable.

Informed consent statement: Not applicable.

Data availability statement: All data supporting the reported results are contained within the article and the cited references. No new datasets were generated during the current study.

Conflict of interest: No conflict of interest was reported by the author.

AI use statement: The author declares that no artificial intelligence (AI) tools were used in the preparation of this manuscript.

References

1. Unnikrishnan R, Shaw JE, Chan JCN, et al. Prediabetes. Nature Reviews Disease Primers. 2025; 11(1): 49. doi: 10.1038/s41572-025-00635-0
2. Lee EH, Lee KH, Lee K, et al. Connection between Impaired Fasting Glucose or Type 2 Diabetes Mellitus and Sepsis: A 10-Year Observational Data from the National Health Screening Cohort. Diabetes & Metabolism Journal. 2025; 49(3): 485–497. doi: 10.4093/dmj.2024.0387
3. Wu H, Lv B, Zhi L, et al. Microbiome–metabolome dynamics associated with impaired glucose control and responses to lifestyle changes. Nature Medicine. 2025; 31(7): 2222–2231. doi: 10.1038/s41591-025-03642-6
4. Bahl V, Rifkind R, Waite E, et al. G6PC2 controls glucagon secretion by defining the set point for glucose in pancreatic α cells. Science Translational Medicine. 2025; 17(779): eadi6148. doi: 10.1126/scitranslmed.adi6148
5. Santillán M. Quantitative Insights into Glucose Regulation: A Review of Mathematical Modeling Efforts. In: Mori Y, Perthame B, Stevens A (editors). Dynamics of Physiological Control. Springer Nature; 2025. pp. 125–148. doi: 10.1007/978-3-031-82396-1_7
6. Wang G. Optimal homeostasis necessitates bistable control. Journal of The Royal Society Interface. 2012; 9(75): 2723–2734. doi: 10.1098/rsif.2012.0244
7. Wang G. Raison d'être of insulin resistance: the adjustable threshold hypothesis. Journal of The Royal Society Interface. 2014; 11(101): 20140892. doi: 10.1098/rsif.2014.0892
8. Akhtar J, Han Y, Han S, et al. Bistable insulin response: The win-win solution for glycemic control. iScience. 2022; 25(12): 105561. doi: 10.1016/j.isci.2022.105561
9. Mitrakou A, Kelley D, Mokan M, et al. Role of Reduced Suppression of Glucose Production and Diminished Early Insulin Release in Impaired Glucose Tolerance. New England Journal of Medicine. 1992; 326(1): 22–29. doi: 10.1056/NEJM199201023260104
10. Bergman RN, Phillips LS, Cobelli C. Physiologic evaluation of factors controlling glucose tolerance in man: measurement of insulin sensitivity and beta-cell glucose sensitivity from the response to intravenous glucose. Journal

of Clinical Investigation. 1981; 68(6): 1456–1467. doi: 10.1172/JCI110398
11. Bergman RN, Ider YZ, Bowden CR, et al. Quantitative estimation of insulin sensitivity. American Journal of Physiology-Endocrinology and Metabolism. 1979; 236(6): E667. doi: 10.1152/ajpendo.1979.236.6.E667
12. DeFronzo RA, Simonson D, Ferrannini E. Hepatic and peripheral insulin resistance: A common feature of Type 2 (non-insulin-dependent) and Type 1 (insulin-dependent) diabetes mellitus. Diabetologia. 1982; 23(4): 313–319. doi: 10.1007/BF00253736
13. Chen YD, Jeng CY, Hollenbeck CB, et al. Relationship between plasma glucose and insulin concentration, glucose production, and glucose disposal in normal subjects and patients with non-insulin-dependent diabetes. Journal of Clinical Investigation. 1988; 82(1): 21–25. doi: 10.1172/JCI113572
14. Purnell JQ, Marshall N, Francisco M, et al. Relationships Between Regional and Ectopic Adiposity and Insulin Sensitivity in Early and Late Pregnancy. Diabetes Care. 2026; 49(7): 1175–1184. doi: 10.2337/dc25-2081
15. Mussnig S, Krenn S, Waller M, et al. Longitudinal patterns of fluid overload, blood volume and vascular refilling: a prospective study in patients on maintenance hemodialysis. Clinical Kidney Journal. 2025; 18(8): sfaf199. doi: 10.1093/ckj/sfaf199
16. Kostamo Z, Ortega MA, Xu C, et al. Base editing HbS to HbG-Makassar improves hemoglobin function supporting its use in sickle cell disease. Nature Communications. 2025; 16(1): 1441. doi: 10.1038/s41467-025-56578-3
17. Muraki R, Hiraoka A, Nagata K, et al. Novel method for estimating the total blood volume: the importance of adjustment using the ideal body weight and age for the accurate prediction of haemodilution during cardiopulmonary bypass. Interactive CardioVascular and Thoracic Surgery. 2018; 27(6): 802–807. doi: 10.1093/icvts/ivy173
18. Matthews DR, Rudenski AS, Burnett MA, et al. The half-life of endogenous insulin and C-peptide in man assessed by somatostatin suppression. Clinical Endocrinology. 1985; 23(1): 71–79. doi: 10.1111/j.1365-2265.1985.tb00185.x
19. Bonadonna RC, Leif G, Kraemer N, et al. Obesity and insulin resistance in humans: A dose-response study. Metabolism. 1990; 39(5): 452–459. doi: 10.1016/0026-0495(90)90002-T
20. Kastrati L, Alvarez-Martinez M, Thomas A, et al. Effect of exercise on plasma insulin levels in individuals with type 1 diabetes: A systematic review and meta-analysis. Diabetes, Obesity and Metabolism. 2025; 27(2): 876–884. doi: 10.1111/dom.16088
21. Topp B, Promislow K, Devries G, et al. A Model of β -Cell Mass, Insulin, and Glucose Kinetics: Pathways to Diabetes. Journal of Theoretical Biology. 2000; 206(4): 605–619. doi: 10.1006/jtbi.2000.2150
22. Malaisse W, Malaisse-Lagae F, Wright PH. A New Method for the Measurement *in Vitro* of Pancreatic Insulin Secretion. Endocrinology. 1967; 80(1): 99–108. doi: 10.1210/endo-80-1-99
23. Neel JV. Diabetes mellitus: a "thrifty" genotype rendered detrimental by "progress"? American Journal of Human Genetics. 1962; 14(4): 353–362.
24. Gugliandolo S, Morciano C, Leccisotti L, et al. Illuminating Glucose: How to Unveil Organ-Specific Insulin Resistance and Guide Metabolic Strategies in Diabetes. Diabetes/Metabolism Research and Reviews. 2026; 42(3): e70162.
25. Zhang Y, Wang C, Zhang P, et al. Mitochondria-associated programmed cell death in pancreatic β cell of T2DM. Apoptosis. 2026; 31(3): 84. doi: 10.1007/s10495-026-02315-0
26. Młynarska E, Czarnik W, Dzieża N, et al. Type 2 Diabetes Mellitus: New Pathogenetic Mechanisms, Treatment and the Most Important Complications. International Journal of Molecular Sciences. 2025; 26(3): 1094. doi: 10.3390/ijms26031094
27. Yang M, Wei Y, Liu J, et al. Contributions of Hepatic Insulin Resistance and Islet β-Cell Dysfunction to the Blood Glucose Spectrum in Newly Diagnosed Type 2 Diabetes Mellitus. Diabetes & Metabolism Journal. 2025; 49(4): 883–892. doi: 10.4093/dmj.2024.0537
28. Chen J, Liu Z, Gu J, et al. Revitalizing p-GSK-3β via cysteine sulfenylation promotes hepatic insulin resistance by differentially regulating glycogenesis and gluconeogenesis. Nature Metabolism. 2026; 8(5): 1173–1188. doi: 10.1038/s42255-026-01507-x
29. Rizza RA. Pathogenesis of Fasting and Postprandial Hyperglycemia in Type 2 Diabetes: Implications for Therapy. Diabetes. 2010; 59(11): 2697–2707. doi: 10.2337/db10-1032
30. Ronald Kahn C. Insulin resistance, insulin insensitivity, and insulin unresponsiveness: A necessary distinction. Metabolism. 1978; 27(12): 1893–1902. doi: 10.1016/S0026-0495(78)80007-9
31. Petersen MC, Shulman GI. Mechanisms of Insulin Action and Insulin Resistance. Physiological Reviews. 2018; 98(4): 2133–2223. doi: 10.1152/physrev.00063.2017
32. Iida H, Watada H. Pancreatic β-cell Dysfunction and Diabetes. Juntendo Medical Journal. 2025; 71(3): 158–165. doi:

10.14789/ejmj.JMJ25-0001-R
33. Bazotte RB, Silva LG, Schiavon FP. Insulin resistance in the liver: Deficiency or excess of insulin? Cell Cycle. 2014; 13(16): 2494–2500. doi: 10.4161/15384101.2014.947750

Appendix A. The Jacobian matrix and its simplification

The Jacobian matrix J at the steady state (G_0, I_0) is

$$J = \begin{bmatrix} -\gamma - V(I_0) & \frac{S'}{\Omega} - V'G_0 \\ f' & -k \end{bmatrix}, \tag{A1}$$

where S', V', and f' denote $\left.\frac{dS_{hep}}{dI}\right|_{I=I_0}$, $\left.\frac{dV}{dI}\right|_{I=I_0}$, and $\left.\frac{df}{dG}\right|_{G=G_0}$, respectively. In Equation (A1), both $V(I_0)$ and V' are approximately zero. This is because the fasting insulin concentration I_0 is far below the insulin activation threshold of insulin-responsive cells, resulting in peripheral tissues extracting negligible blood glucose in the fasting state—that is, $V(I_0) \approx 0$. This $V(I) \approx 0$ applies not only to the single point I_0 but also to a wide range of insulin concentrations encompassing I_0 (see the flat region around the black point in **Figure 1a**). Therefore, $V' \approx 0$. Taken together, the Jacobian matrix J reduces to Equation (8).

Appendix B. The variation in Δ is primarily attributable to $\widehat{\alpha}$, i_0, and g_0

To simplify the expression of Δ, we first need to better present the change in S'. To this end, Equation (15) is converted into

$$S' = -\widehat{\alpha}\frac{S_{basal}}{I_{basal}} exp\left[-\widehat{\alpha}\left(i_0 - 1\right)\right], \tag{A2}$$

where $i_0 = \frac{I_0}{I_{basal}}$ and $\widehat{\alpha} = \alpha I_{basal}$. Compared with S_{basal} and I_{basal}, $\widehat{\alpha}$ and i_0 have larger magnitudes of variation, so they are selected as adjustable parameters.

We then need to better present the change in f'. To this end, Equation (16) is converted into

$$f' = \frac{n f_{max} \mathrm{Hill}\left(g_0\right)\left[1 - \mathrm{Hill}\left(g_0\right)\right]}{g_0 G_h}, \tag{A3}$$

where $g_0 = \frac{G_0}{G_h}$. The function $f'(g_0)$ is shown in **Figure 1d**. Compared with n, $f_{\max}$, and G_h, g_0 has a larger magnitude of variation, so it is selected as an adjustable parameter.

Taken together, the determinant Δ has three adjustable parameters: $\widehat{\alpha}$, i_0, and g_0. Other parameters of Δ take fixed values from **Table 2**. Thus we obtain Equation (17).